Many-Body Interference at the Onset of Chaos

Eric Brunner[1,2,*] Lukas Pausch[1,2,†] Edoardo G. Carnio[1,2] Gabriel Dufour[1,2]
Alberto Rodríguez[3,4] and Andreas Buchleitner[1,2]

[1]*Physikalisches Institut, Albert-Ludwigs-Universität Freiburg, Hermann-Herder-Straße 3, 79104, Freiburg, Germany*
[2]*EUCOR Centre for Quantum Science and Quantum Computing, Albert-Ludwigs-Universität Freiburg,*
Hermann-Herder-Straße 3, 79104, Freiburg, Germany
[3]*Departamento de Física Fundamental, Universidad de Salamanca, E-37008 Salamanca, Spain*
[4]*Instituto Universitario de Física Fundamental y Matemáticas (IUFFyM), Universidad de Salamanca, E-37008 Salamanca, Spain*

We unveil the signature of many-body interference across dynamical regimes of the Bose-Hubbard model. Increasing the particles' indistinguishability enhances the temporal fluctuations of few-body observables, with a dramatic amplification at the onset of quantum chaos. By resolving the exchange symmetries of partially distinguishable particles, we explain this amplification as the fingerprint of the initial state's coherences in the eigenbasis.

Interacting many-particle dynamics may be considered *the* most plausible origin of instabilities, chaos, and complexity, from astronomical [1,2] to microscopic [3] scales. Because of the rapid growth of phase space with the particle number, together with its progressively more intricate topology, deterministic descriptions quickly hit the ceiling, enforcing statistical descriptions. Some type of coarse graining, implicit to such approaches, allows classifications of dynamical behavior—e.g., as scale invariant, chaotic, or Markovian—associated with *universal* characteristics that are formalized, e.g., in the theories of phase transitions [4,5], random matrices (RMT) [6], or open quantum systems [7–9]. It is the universal character of these features that allows robust predictions, since full resolution of complex dynamics is prohibitive, by their very nature.

On the quantum level, robust features are in such scenarios essentially controlled by spectral densities and statistics, the localization properties of eigen- and initial states, the phase-space dimension, and the timescales over which to make predictions. This is the unifying view of quantum chaos [10], which has proven enormously versatile an approach to analyze complex quantum systems—including paradigmatic many-particle scenarios in nuclear [11,12] and atomic physics [13–15], as well as in cold matter [16–19] and black hole [20] contexts. On this level of description, the specific many-particle nature of the underlying Hamiltonian does not appear as an essential ingredient anymore, since all the features of complex dynamics can also be observed on the level of single-particle dynamics [10,21] (provided the phase-space dimension is large enough—such that tori are not isolating anymore [22]).

Yet, quantum systems composed of identical particles undeniably exhibit properties that fundamentally distinguish them from classical many- and single-particle systems,

hardwired in exchange symmetries [23,24], and generating many-body interference (MBI) phenomena [25–38], thus with potentially dramatic dynamical relevance. In fact, modern experiments [19,39–47] already allow one to control external and internal degrees of freedom (d.o.f.) of many-particle quantum systems, such that physically identical particles may be equipped with a continuously tunable degree of partial distinguishability (PD), and, by this, to ultimately control the impact of MBI on the dynamics [32,34–36]. While, traditionally, the RMT approach deliberately divides out any symmetry-induced properties [6,10] (see, however, [48]), it is clear that MBI, as a manifestation of the specific system's particle-exchange symmetry, is one of those robust features that need to be accounted for in any theory of complex quantum systems. This raises the question: Where in a many-body quantum system's spectral and eigenstate structure is MBI encoded and how can we distill its impact on observable dynamical properties?

In this contribution, we identify a signature of bosonic MBI in the asymptotic temporal fluctuations v of expectation values around their average. We show that v is controlled by the coherences of the many-particle initial state in the eigenbasis, multiplied by the corresponding off-diagonal elements of the observable, and is therefore strongly enhanced by particle indistinguishability. We extract v from the quench dynamics of a Mott state in the Bose-Hubbard model for increasing values of tunneling strength J. As shown in Fig. 1, v is sharply peaked around the value of J where the dynamics becomes chaotic. There, the initial state is sufficiently delocalized in the eigenbasis for coherences to build up, but not so much that they are cut off by the finite energy bandwidth of the observable. By taking into account the eigenstates' structure as constrained by their symmetry under particle exchange, we find

the strongest dependence of v on the particles' mutual (in)distinguishability precisely at that point. Given the very general ingredients of our theoretical analysis, we conclude that many-body coherence effects are most intense at the onset of quantum chaos.

We consider the one-dimensional Bose-Hubbard model [40,49–52] of PD particles with hard-wall boundary conditions,

$$H = -J \sum_{\langle i,j \rangle} \sum_{\sigma=1}^{s} a_{i\sigma}^{\dagger} a_{j\sigma} + \frac{U}{2} \sum_{i=1}^{L} N_i(N_i - 1), \quad (1)$$

which is experimentally realizable with ultracold atoms in optical lattices [19,39–47]. The first index of the creation and annihilation operators $a_{i\sigma}^{\dagger}, a_{j\sigma}$ refers to the L Wannier orbitals of the lattice, which span the *external* single-particle Hilbert space $\mathcal{H}_{\text{ext}}$. The second index σ refers to a basis of the s-dimensional *internal* single-particle Hilbert space, describing, e.g., the electronic state of an atom loaded into an optical lattice. The operator $N_i = \sum_{\sigma=1}^{s} a_{i\sigma}^{\dagger} a_{i\sigma}$ counts the number of particles on lattice site i, irrespective of their internal state. We keep the total particle number $N = \sum_{i=1}^{L} N_i$ fixed. The two terms in H describe nearest-neighbor tunneling and on-site interaction of the particles, both of which act exclusively on the external d.o.f., while the internal d.o.f. remain static. For indistinguishable bosons, depending on the relative contribution of both terms in (1), a quantum-chaotic region has been identified both from spectral statistics and eigenstate delocalization [19,46,47,53–61]. We here establish its existence also for PD particles, as an important corollary of our subsequent analysis.

Of experimental interest are few-particle observables, e.g., low-order density correlations $O = N_i N_j$. Formally, these are given by products of k creation and k annihilation operators [32,34], $k \ll N$, such that they only access the marginal information inscribed in the k-particle (kP) reduced state [36,62]. Moreover, like the Hamiltonian, these observables are assumed to exclusively act on external d.o.f., such that we can consider their restriction to $\mathcal{H}_{\text{ext}}^{\otimes N}$ and trace out the internal d.o.f. from the full system state ϱ to obtain $\rho = \text{tr}_{\text{int}}\varrho$ [35,36,62]. Partial distinguishability of the particles results in entanglement between their external and internal d.o.f. [35,36], and we use as a measure of indistinguishability the purity $\gamma = \text{tr}\rho^2$ of the external state, which is maximal ($\gamma = 1$) for indistinguishable particles and minimal for perfectly distinguishable ones [35,62].

The system's dynamical equilibration, on asymptotic timescales, is captured by the temporal variance of expectation values $\langle O(t) \rangle$,

$$\text{Var}_t[O] = \overline{\langle O(t) \rangle^2} - \overline{\langle O(t) \rangle}^2, \quad (2)$$

where $\overline{\cdots}$ indicates the average over the positive time axis (see Supplemental Material [63]). To formulate general statements, independent of the specific choice of observable
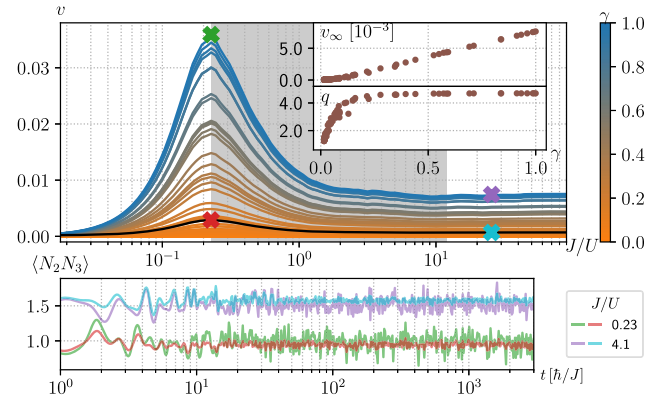

FIG. 1. Fluctuations of two-particle observables in the Bose-Hubbard model (1) for $N = L = 6$. Top: average temporal variance v [Eq. (3)] versus J/U, for 100 initial states with one particle per site and variable particle indistinguishability γ (color bar). The black curve highlights the case analyzed in Fig. 2(b). The gray-shaded area indicates the quantum-chaotic region of (1) [also see Figs. 2(b) and 2(c)]. Insets show the plateau value v_∞ (large J/U) and the enhancement $q = v_{\max}/v_\infty$ of the maximal fluctuation $v_{\max}$, as functions of γ. Bottom: time series of $\langle N_2(t)N_3(t) \rangle$ for four combinations of J/U and γ (identified by correspondingly colored crosses in the top panel). For visibility, the curves for $J/U = 4.1$ are shifted upward by 0.8.

O, we consider an unbiased average (indicated by $\widehat{\cdots}$) over an orthonormal basis $\mathcal{B}$ of the (finite-dimensional) Hilbert space of external kP observables [64],

$$v := \widehat{\text{Var}_t[O]} = \sum_{o \in \mathcal{B}} \text{Var}_t[o]. \quad (3)$$

This quantity is shown, for $k = 2$, in Fig. 1 (top panel), for the dynamics generated by (1), with $N = L = 6$, initially one particle per external mode, versus the control parameter J/U. A variable level of PD is obtained by random generation [63] of the particles' internal states $|\phi_i\rangle = \sum_\sigma \phi_{i\sigma}|\sigma\rangle$, $i = 1, ..., L$, of the initial Mott state, such as to smoothly cover the entire range $\gamma \in [1/N!; 1]$.

We observe that, for all J/U, v monotonically grows with γ, i.e., as MBI contributions are enhanced. Moreover, v exhibits a maximum $v_{\max}$ at $J/U \simeq 0.23$ and then decreases to a plateau value v_∞ with increasing J/U. The peak is located at the transition to the (gray-shaded) parameter range where (1) exhibits fully developed quantum chaos, as identified by the ergodicity properties of its eigenstates [see discussion of Fig. 2(c) below]. Both v_∞ and the enhancement $q = v_{\max}/v_\infty$ of the fluctuations at the peak increase monotonically with γ, as shown in the inset. In particular, q steeply increases at small γ, when MBI starts to kick in, which signals a particularly strong sensitivity to MBI at the transition to quantum chaos. We observe the same qualitative behavior (see Supplemental Material [63]) for the experimentally more accessible average $\sum_{i \neq j} \text{Var}_t[N_i N_j]$ over all two-point density correlations [29,65]. In the bottom panel of Fig. 1, we also give
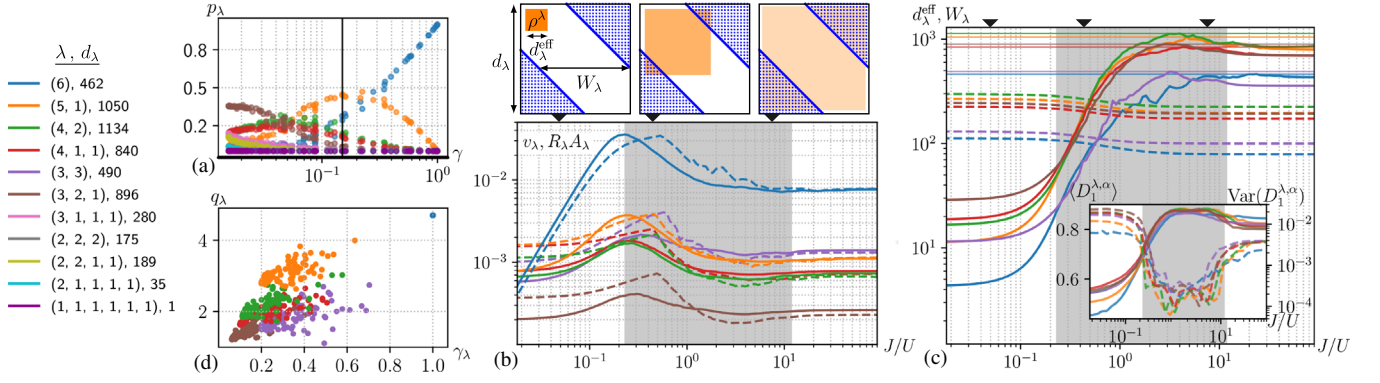
FIG. 2. Ingredients determining the averaged temporal variance v shown in Fig. 1, as functions of J/U and of the particles' indistinguishability γ. The legend color codes the symmetry sectors λ and indicates their corresponding block dimensions d_λ. (a) Weights p_λ [see Eq. (4)] of the initial states for varying γ (vertical black line marks $\gamma = 0.15$). (b) Bottom: comparison of v_λ (solid), Eq. (4), to the factorized approximation $R_\lambda A_\lambda$ (dashed), Eq. (5), versus J/U, for $\gamma \simeq 0.15$. Top: qualitative illustration of the competition between the delocalization d_λ^{eff} of the initial state's component ρ^λ and the bandwidth W_λ of the averaged observable $|\widehat{O_{\alpha\beta}^\lambda}|^2$, in the eigenbasis of the symmetry sector λ, for three values of J/U. (c) Evolution of W_λ (dashed) and d_λ^{eff} (solid) with J/U (horizontal lines highlight block dimensions d_λ). Inset: delocalization of the 60 eigenstates closest in energy to the initial state, quantified by the mean value (solid) and variance (dashed) of their fractal dimensions with respect to the Young basis, identifying the chaotic phase [shaded regions in the inset and in the main panels of (b) and (c)]. (d) Distribution of the sector-specific enhancement q_λ for initial states with variable γ_λ. For clarity, (b)–(d) show data for the largest six sectors only.

the long-time series of $\langle N_2(t)N_3(t)\rangle$, for four values of J/U and γ, with strongest fluctuations for intermediate $J/U \simeq 0.23$ and $\gamma = 1$, in agreement with the above. The peak in the fluctuations at the onset of chaos can be qualitatively explained by the competition between the initial state's delocalization and the observable's bandwidth in the eigenbasis, as sketched in the top panels of Fig. 2(b). However, a precise discussion requires one to first consider the particle-exchange symmetry of PD bosons, which is at the origin of the overall increase of v with indistinguishability γ.

States of PD bosons are characterized by the coexistence of several types of mixed particle-exchange symmetries, alongside the fully symmetric, bosonic symmetry [24,34]. The suppression of v as we make particles more distinguishable (i.e., for decreasing γ) can be understood by the emergence of such nonbosonic contributions to the dynamics. Indeed, group representation theory, and specifically the Schur-Weyl duality [66,67], tell us that H, O, and ρ (as operators on $\mathcal{H}_{\text{ext}}^{\otimes N}$) decompose into symmetry sectors labeled by the integer partitions of N (or Young diagrams): $\lambda = (N), (N-1,1), (N-2,2), \ldots, (1,1,\ldots)$. While states ρ of perfectly indistinguishable bosons are entirely supported on the *bosonic* sector, $\lambda = (N)$, states of PD particles also have finite weights p_λ on the other sectors ($\sum_\lambda p_\lambda = 1$), as shown in Fig. 2(a) for states with variable levels of indistinguishability γ (as used as initial states in Fig. 1). Every sector further decomposes [63] into ν_λ identical blocks, each of dimension d_λ, and we denote by $\{|\lambda, m\rangle\}_{m=1,\ldots,d_\lambda}$ the Young basis [34,66], built upon the Wannier basis, of one such block. Diagonalizing H in this very block, we find the eigenstates

$|E_\alpha^\lambda\rangle = \sum_{m=1}^{d_\lambda} c_{\alpha m}^\lambda |\lambda, m\rangle$, with respect to which we represent the observable and the initial state, $O_{\alpha\beta}^\lambda = \langle E_\alpha^\lambda | O | E_\beta^\lambda \rangle$ and $\rho_{\alpha\beta}^\lambda = \nu_\lambda \langle E_\alpha^\lambda | \rho | E_\beta^\lambda \rangle / p_\lambda$. With this definition, the matrix ρ^λ has unit trace. If we denote its purity by $\gamma_\lambda = \text{tr}[(\rho^\lambda)^2]$, the purity of ρ reads $\gamma = \sum_\lambda p_\lambda^2 \gamma_\lambda / \nu_\lambda$.

The above structure allows to decompose v, as given by Eq. (3), into contributions from individual symmetry sectors. In the absence of degeneracies between energy levels and between energy gaps, within each block and between λ sectors, we obtain [63]

$$v = \sum_\lambda p_\lambda^2 v_\lambda, \qquad v_\lambda = \sum_{\alpha \neq \beta} |\rho_{\alpha\beta}^\lambda|^2 |\widehat{O_{\alpha\beta}^\lambda}|^2. \qquad (4)$$

The individual contributions are determined by the *squared* weights p_λ^2 and by the *off-diagonal* elements $|\rho_{\alpha\beta}^\lambda|^2$, $|\widehat{O_{\alpha\beta}^\lambda}|^2$ of initial state and observable in the eigenbasis. For indistinguishable particles, $\gamma = 1$ and $p_\lambda = \delta_{\lambda,(N)}$, the fluctuations $v = v_{(N)}$ are thus governed by purely bosonic MBI. As γ decreases, the state starts to distribute over other sectors, as shown in Fig. 2(a). The fluctuations v are then doubly suppressed: through the squared weights p_λ^2 in Eq. (4), and because of $v_\lambda \leq v_{(N)}$ for all λ, as we will show in Fig. 2(b). In the limit of distinguishable particles (smallest $\gamma = 1/N!$), the state is distributed over all sectors and v is minimal.

To elucidate the origin of the maximum of v at the transition to quantum chaos, we develop a simple statistical model for the off-diagonal elements of state and observable appearing in Eq. (4). We assume that the averaged matrix

elements $|\widehat{O^\lambda_{\alpha\beta}}|^2$ vanish outside a band of width W_λ [63,68], as suggested by the eigenstate thermalization hypothesis [69–74]. As for the state ρ^λ, we suppose that it only populates d^{eff}_λ consecutive (in energy) eigenstates, as sketched in the top panels of Fig. 2(b). Otherwise, $|\rho^\lambda_{\alpha\beta}|^2$ and $|\widehat{O^\lambda_{\alpha\beta}}|^2$ are assumed to be statistically independent, such that we can factorize (see Supplemental Material [63])

$$v_\lambda \approx R_\lambda A_\lambda, \qquad R_\lambda = \frac{\sum_{\alpha\neq\beta}|\rho^\lambda_{\alpha\beta}|^2}{\max(d^{\text{eff}}_\lambda, W_\lambda)},$$

$$A_\lambda = \frac{\sum_{\alpha\neq\beta}|\widehat{O^\lambda_{\alpha\beta}}|^2}{d_\lambda}. \tag{5}$$

This is qualitatively underpinned by Fig. 2(b), for a state with $\gamma = 0.15$, for the largest six symmetry sectors (which carry 99.2% of ρ). Note that weighting those v_λ by the squares of the associated p_λ [black vertical line in Fig. 2(a)] according to Eq. (4) results in the black curve highlighted in the upper panel of Fig. 1.

We find that A_λ is, to a good approximation, independent of J/U and of order 1 in all contributing sectors [63,75]. Consequently, the dependence of v_λ on J/U is predominantly controlled by R_λ. From R_λ [cf. Eq. (5)], we rewrite the sum over coherences $\sum_{\alpha\neq\beta}|\rho^\lambda_{\alpha\beta}|^2 = \gamma_\lambda - I_\lambda$, where the inverse participation ratio $I_\lambda = \sum_\alpha |\rho^\lambda_{\alpha\alpha}|^2$ is a measure of the initial state's localization in the eigenbasis, to which we now turn.

Since I^{-1}_λ provides an estimate of the number of eigenstates occupied by the initial state, we use it to define the state's effective dimension $d^{\text{eff}}_\lambda = C_\lambda/I_\lambda$. The multiplicative factor C_λ enforces $d^{\text{eff}}_\lambda \to d_\lambda$ in the regime of strongest delocalization, since, due to residual fluctuations of $\rho_{\alpha\alpha}$, I^{-1}_λ generically underestimates the actual number of populated eigenstates. Figure 2(c) illustrates the delocalization of the initial state seeding the fluctuations displayed in Fig. 1, in the energy eigenbasis of the largest six sectors [carrying between 68% (distinguishable particles) and 100% (indistinguishable particles) of the initial state, cf. Fig. 2(a)]. From the strongly interacting limit $J/U \to 0$, d^{eff}_λ grows with increasing tunneling strength, reaching a maximum in most sectors in the range $J/U \in [3; 4]$, before stabilizing at a value of order d_λ for $J/U \to \infty$.

The delocalization of the initial state in the eigenbasis mirrors the delocalization of the eigenstates in the Young basis $\{|\lambda, m\rangle\}_{m=1,\dots,d_\lambda}$, which signals the emergence of quantum chaos. As demonstrated in Refs. [59–61] for indistinguishable bosons, the chaotic region can be identified by the ergodicity of eigenstates in the individual λ sectors, as measured by their fractal dimension $D^{\lambda,\alpha}_1 = -\sum^{d_\lambda}_{m=1}|c^\lambda_{\alpha m}|^2 \log_{d_\lambda}|c^\lambda_{\alpha m}|^2$. The inset of Fig. 2(c) shows the mean value $\langle D^{\lambda,\alpha}_1 \rangle$ and the variance $\text{Var}(D^{\lambda,\alpha}_1)$,

taken over the 60 eigenstates closest in energy to the initial state, for each λ sector. A substantial delocalization occurs for $0.23 \lesssim J/U \lesssim 11$ (shaded area), where the mean values reach their maxima, accompanied by a drop of the variances by at least 1 order of magnitude, attesting a strongly uniform eigenstate structure in all shown sectors. Consequently, the chaotic domain identified for indistinguishable bosons [59] persists for mixed particle-exchange symmetry.

In contrast to the sharp growth of d^{eff}_λ, the bandwidth W_λ of the observable only decreases slightly with J/U. We estimate it by taking the standard deviation of the (normalized) distribution $f_\alpha(\beta) \propto |\widehat{O^\lambda_{\alpha\beta}}|^2$ for each α and averaging over α. Figure 2(c) shows the resulting W_λ (dashed lines) versus J/U, in the largest six sectors.

The behavior of v_λ can then be qualitatively understood in terms of the three regimes sketched at the top of Fig. 2(b). In the limit $J/U \to 0$ (leftmost sketch), the initial Mott state is itself an eigenstate and decomposes on only a few (degenerate) eigenstates $|E^\lambda_\alpha\rangle$. Accordingly, the inverse participation ratio is maximal, yielding a minimal value of the sum over coherences $\gamma_\lambda - I_\lambda$, as captured by the decreasing left tails of the v_λ in Fig. 2(b). Instead, for J/U within and beyond the range of fully developed quantum chaos (rightmost sketch), the initial state is strongly delocalized in the eigenbasis ($d^{\text{eff}}_\lambda \approx d_\lambda$), such that many nonzero coherences $|\rho^\lambda_{\alpha\beta}|^2$ with $|\alpha - \beta| > W^\lambda$ are suppressed by multiplication with a vanishing $|\widehat{O^\lambda_{\alpha\beta}}|^2$ in Eq. (4). In the factorized form Eq. (5), this effect gives rise to the denominator $\max(d^{\text{eff}}_\lambda, W_\lambda)$ of R_λ, which results (with $I_\lambda \ll \gamma_\lambda$, $d^{\text{eff}}_\lambda \approx d_\lambda > W_\lambda$) in a small asymptotic value $R^\infty_\lambda \approx \gamma_\lambda/d_\lambda \ll 1$ for large J/U. At the transition between the two parameter ranges (central sketch), the onset of quantum chaos, where the eigenstates undergo a metamorphosis from localized to ergodic, triggers the initial state's delocalization in the eigenbasis. There, R_λ exhibits a maximum, since ρ^λ already populates a substantial energy window, resulting in an enhanced contribution by coherences, which are, however, not yet suppressed by the observable's bandwidth.

To explain why the effect of PD on v is comparatively strongest at this maximum, we turn to the dependence of v_λ on the purity γ_λ of the state ρ^λ associated with a given symmetry sector: We have seen that the plateau value $v^\infty_\lambda \sim R^\infty_\lambda$ scales linearly with γ_λ. In Fig. 2(d), we observe a correlation of the sector-specific enhancement $q_\lambda = v^{\max}_\lambda/v^\infty_\lambda$ with γ_λ (for those sectors contributing most), signaling a faster-than-linear scaling of the peak height $v^{\max}_\lambda$ with γ_λ. Accordingly, the relative peak height q_λ is largest for the bosonic sector $\lambda = (N)$, which always has maximal purity $\gamma_{(N)} = 1$ [63]. This explains the sharp growth of q observed in the inset of Fig. 1 for $0 \lesssim \gamma \lesssim 0.2$, as the bosonic contribution to v in Eq. (4) surpasses

contributions from nonbosonic sectors [Figs. 2(a) and 2(b)]. For $\gamma \gtrsim 0.4$, the bosonic contribution is dominant, as reflected by the convergence of q toward $q_{(N)}$ [cf. inset Fig. 1].

We have thus shown that many-body coherences populated by the initial state leave a statistically robust imprint in the long-time fluctuations of few-particle observables. The emergence of the chaotic phase induces the delocalization of the initial state in the eigenbasis, translating into an augmented contribution of coherences within the observable's energy bandwidth, and hence leading to the maximization of fluctuations. This reflects the enhanced sensitivity of a quantum system's eigenstate structure (anchored in the underlying phase-space's topological metamorphosis [10]) at the chaos transition, which is inherited by single-particle as well as by many-particle transition amplitudes [76–78]. While this fluctuation maximum is observed for any degree of particle distinguishability, it is significantly amplified as the particles become more indistinguishable, because of many-body interference contributions stemming from the bosonic symmetry sector. Therefore, full resolution of the particle-exchange symmetry sectors is indispensable to understand how MBI is seeded by the spectral and eigenstate structure of a many-body quantum system and to discern MBI's impact on the dynamics. Ultimately, this approach allows the discrimination of interaction induced from entirely quantum (due to many-particle interferences) causes of dynamical complexity.

---

*eric.brunner@physik.uni-freiburg.de

†Present address: CESAM Research Unit, University of Liège, 4000 Liège, Belgium.

[1] B. Chirikov and V. Vecheslavov, Astron. Astrophys. **221**, 146 (1989), https://ui.adsabs.harvard.edu/abs/1989A%26A...221..146C/abstract.

[2] J. Laskar and M. Gastineau, Nature (London) **459**, 817 (2009).

[3] N. Bohr, Nature (London) **137**, 344 (1936).

[4] L. Landau and E. Lifschitz, *Lehrbuch der Theoretischen Physik, Band V: Statistische Physik, Teil 1* (Akademie-Verlag, Berlin, 1984).

[5] S. Sachdev, *Quantum Phase Transitions* (Cambridge University Press, Cambridge, England, 2011).

[6] M. L. Mehta, *Random Matrices*, 3rd ed. (Elsevier, Amsterdam, 1991), 10.1016/C2009-0-22297-5.

[7] E. Davies, *Quantum Theory of Open Quantum Systems* (Academic Press, New York, 1976).

[8] R. Alicki and K. Lendi, *Quantum Dynamical Semigroups and Applications* (Springer Verlag, Berlin, 1987), 10.1007/3-540-18276-4.

[9] H.-P. Breuer and F. Petruccione, *The Theory of Open Quantum Systems* (Cambridge University Press, Cambridge, England, 2002).

[10] *Les Houches Session LII: Chaos and Quantum Physics*, edtited by M. J. Giannoni, A. Voros, and J. Zinn-Justin (North-Holland, Amsterdam, 1989).

[11] T. Guhr and H. A. Weidenmüller, Ann. Phys. (N.Y.) **193**, 472 (1989).

[12] I. Rotter, Rep. Prog. Phys. **54**, 635 (1991).

[13] A. Holle, J. Main, G. Wiebusch, H. Rottke, and K. H. Welge, Phys. Rev. Lett. **61**, 161 (1988).

[14] C. H. Iu, G. R. Welch, M. M. Kash, D. Kleppner, D. Delande, and J. C. Gay, Phys. Rev. Lett. **66**, 145 (1991).

[15] A. Krug and A. Buchleitner, Phys. Rev. Lett. **86**, 3538 (2001).

[16] F. L. Moore, J. C. Robinson, C. F. Bharucha, B. Sundaram, and M. G. Raizen, Phys. Rev. Lett. **75**, 4598 (1995).

[17] S. Wimberger, I. Guarneri, and S. Fishman, Phys. Rev. Lett. **92**, 084102 (2004).

[18] F. Meinert, M. J. Mark, E. Kirilov, K. Lauber, P. Weinmann, M. Gröbner, and H.-C. Nägerl, Phys. Rev. Lett. **112**, 193003 (2014).

[19] A. M. Kaufman, M. E. Tai, A. Lukin, M. Rispoli, R. Schittko, P. M. Preiss, and M. Greiner, Science **353**, 794 (2016).

[20] H. Liu and S. Vardhan, J. High Energy Phys. 03 (2021) 088.

[21] R. Garbaczewski and R. Olkiewicz, eds., *Dynamics of Dissipation* (Springer Verlag, Berlin, 2002).

[22] J. von Milczewski, G. H. F. Diercksen, and T. Uzer, Phys. Rev. Lett. **76**, 2890 (1996).

[23] L. Landau and E. Lifschitz, *Lehrbuch der Theoretischen Physik, Band III: Quantenmechanik* (Akademie-Verlag, Berlin, 1985).

[24] M. C. Tichy and K. Mølmer, Phys. Rev. A **96**, 022119 (2017).

[25] C. K. Hong, Z. Y. Ou, and L. Mandel, Phys. Rev. Lett. **59**, 2044 (1987).

[26] M. C. Tichy, M. Tiersch, F. de Melo, F. Mintert, and A. Buchleitner, Phys. Rev. Lett. **104**, 220405 (2010).

[27] G. Dufour, T. Brünner, C. Dittel, G. Weihs, R. Keil, and A. Buchleitner, New J. Phys. **19**, 125015 (2017).

[28] V. S. Shchesnovich and M. E. O. Bezerra, Phys. Rev. A **98**, 033805 (2018).

[29] T. Giordani, F. Flamini, M. Pompili, N. Viggianiello, N. Spagnolo, A. Crespi, R. Osellame, N. Wiebe, M. Walschaers, A. Buchleitner, and F. Sciarrino, Nat. Photonics **12**, 173 (2018).

[30] C. Dittel, G. Dufour, M. Walschaers, G. Weihs, A. Buchleitner, and R. Keil, Phys. Rev. Lett. **120**, 240404 (2018).

[31] C. Dittel, G. Dufour, M. Walschaers, G. Weihs, A. Buchleitner, and R. Keil, Phys. Rev. A **97**, 062116 (2018).

[32] T. Brünner, G. Dufour, A. Rodríguez, and A. Buchleitner, Phys. Rev. Lett. **120**, 210401 (2018).

[33] A. E. Jones, A. J. Menssen, H. M. Chrzanowski, T. A. W. Wolterink, V. S. Shchesnovich, and I. A. Walmsley, Phys. Rev. Lett. **125**, 123603 (2020).

[34] G. Dufour, T. Brünner, A. Rodríguez, and A. Buchleitner, New J. Phys. **22**, 103006 (2020).

[35] C. Dittel, G. Dufour, G. Weihs, and A. Buchleitner, Phys. Rev. X **11**, 031041 (2021).

[36] E. Brunner, A. Buchleitner, and G. Dufour, Phys. Rev. Res. **4**, 043101 (2022).

[37] M. C. Tichy, J. F. Sherson, and K. Mølmer, Phys. Rev. A **86**, 063630 (2012).

[38] S. Stanisic and P. S. Turner, Phys. Rev. A **98**, 043839 (2018).

[39] M. Greiner, O. Mandel, T. Esslinger, T. W. Hänsch, and I. Bloch, Nature (London) **415**, 39 (2002).

[40] I. Bloch, J. Dalibard, and W. Zwerger, Rev. Mod. Phys. **80**, 885 (2008).

[41] T. Gericke, P. Würtz, D. Reitz, T. Langen, and H. Ott, Nat. Phys. **4**, 949 (2008).

[42] N. Gemelke, X. Zhang, C.-L. Hung, and C. Chin, Nature (London) **460**, 995 (2009).

[43] M. Karski, L. Förster, J. M. Choi, W. Alt, A. Widera, and D. Meschede, Phys. Rev. Lett. **102**, 053001 (2009).

[44] W. S. Bakr, A. Peng, M. E. Tai, R. Ma, J. Simon, J. I. Gillen, S. Folling, L. Pollet, and M. Greiner, Science **329**, 547 (2010).

[45] J. F. Sherson, C. Weitenberg, M. Endres, M. Cheneau, I. Bloch, and S. Kuhr, Nature (London) **467**, 68 (2010).

[46] A. Lukin, M. Rispoli, R. Schittko, M. E. Tai, A. M. Kaufman, S. Choi, V. Khemani, J. Léonard, and M. Greiner, Science **364**, 256 (2019).

[47] M. Rispoli, A. Lukin, R. Schittko, S. Kim, M. E. Tai, J. Léonard, and M. Greiner, Nature (London) **573**, 385 (2019).

[48] O. Giraud, N. Macé, É. Vernier, and F. Alet, Phys. Rev. X **12**, 011006 (2022).

[49] M. P. A. Fisher, P. B. Weichman, G. Grinstein, and D. S. Fisher, Phys. Rev. B **40**, 546 (1989).

[50] M. Lewenstein, A. Sanpera, V. Ahufinger, B. Damski, A. Sen(De), and U. Sen, Adv. Phys. **56**, 243 (2007).

[51] M. A. Cazalilla, R. Citro, T. Giamarchi, E. Orignac, and M. Rigol, Rev. Mod. Phys. **83**, 1405 (2011).

[52] K. V. Krutitsky, Phys. Rep. **607**, 1 (2016).

[53] A. Buchleitner and A. R. Kolovsky, Phys. Rev. Lett. **91**, 253002 (2003).

[54] A. R. Kolovsky and A. Buchleitner, Europhys. Lett. **68**, 632 (2004).

[55] C. Kollath, G. Roux, G. Biroli, and A. M. Läuchli, J. Stat. Mech. (2010) P08011.

[56] W. Beugeling, A. Andreanov, and M. Haque, J. Stat. Mech. (2015) P02002.

[57] R. Dubertrand and S. Müller, New J. Phys. **18**, 033009 (2016).

[58] W. Beugeling, A. Bäcker, R. Moessner, and M. Haque, Phys. Rev. E **98**, 022204 (2018).

[59] L. Pausch, E. G. Carnio, A. Rodríguez, and A. Buchleitner, Phys. Rev. Lett. **126**, 150601 (2021).

[60] L. Pausch, E. G. Carnio, A. Buchleitner, and A. Rodríguez, New J. Phys. **23**, 123036 (2021).

[61] L. Pausch, A. Buchleitner, E. G. Carnio, and A. Rodríguez, J. Phys. A **55**, 324002 (2022).

[62] E. Brunner, Many-body interference, partial distinguishability and entanglement, M.Sc. thesis, Albert-Ludwigs-Universität Freiburg, 2019, https://freidok.uni-freiburg.de/data/166467.

[63] See Supplemental Material at http://link.aps.org/supplemental/10.1103/PhysRevLett.130.080401 for a brief description of the sampling of the particles' internal states (Figs. 1 and 2), a comparison between the average (3) and the average over two-point density correlators, a short summary of the Schur-Weyl duality and the derivations of Eqs. (4) and (5), a discussion of the banded structure and of the average matrix elements of the observable in the eigenbasis, as well as its contribution to Eq. (5).

[64] Note that v is independent of the chosen operator basis.

[65] M. Walschaers, J. Kuipers, J.-D. Urbina, K. Mayer, M. C. Tichy, K. Richter, and A. Buchleitner, New J. Phys. **18**, 032001 (2016).

[66] W. Fulton and J. Harris, *Representation Theory* (Springer, New York, 2004), 10.1007/978-1-4612-0979-9.

[67] D. J. Rowe, M. J. Carvalho, and J. Repka, Rev. Mod. Phys. **84**, 711 (2012).

[68] Note that $|\widehat{O^\lambda_{\alpha\beta}}|^2 \propto \mathrm{tr}_{N-k}[\varepsilon^{\lambda,N-k}_\alpha \varepsilon^{\lambda,N-k}_\beta]$, with $\varepsilon^{\lambda,N-k}_\alpha = \mathrm{tr}_k[|E^\lambda_\alpha\rangle\langle E^\lambda_\alpha|]$ the $(N-k)$P reduced eigenstates [63]. A banded structure of $|\widehat{O^\lambda_{\alpha\beta}}|^2$ thus implies a rapid transition from almost parallel to almost orthogonal (with respect to the Hilbert-Schmidt inner product) reduced eigenstates $\varepsilon^{\lambda,N-k}_\alpha$, with increasing $|\alpha-\beta|$. A loss of eigenstate orthogonality upon tracing over a kP subset implies entanglement between that subset and the remainder.

[69] M. Feingold and A. Peres, Phys. Rev. A **34**, 591 (1986).

[70] J. M. Deutsch, Phys. Rev. A **43**, 2046 (1991).

[71] M. Srednicki, Phys. Rev. E **50**, 888 (1994).

[72] M. Srednicki, J. Phys. A **32**, 1163 (1999).

[73] M. Hiller, T. Kottos, and T. Geisel, Phys. Rev. A **73**, 061604 (R) (2006).

[74] J. M. Deutsch, Rep. Prog. Phys. **81**, 082001 (2018).

[75] The sum over all modulus-squared matrix elements of an operator yields its (basis-independent) squared Hilbert-Schmidt norm. Therefore the sums over off-diagonal elements appearing in Eq. (5) behave complementarily to the sums over diagonal elements as J/U is varied. For few-body observables, the latter, $\sum_\alpha |\widehat{O^\lambda_{\alpha\alpha}}|^2$, is expected to vary only slightly with J/U, since expectation values in all eigenstates remain of the same order.

[76] J. M. Robbins, Phys. Rev. A **40**, 2128 (1989).

[77] T. H. Seligman and H. A. Weidenmüller, J. Phys. A **27**, 7915 (1994).

[78] P. Schlagheck, D. Ullmo, J. D. Urbina, K. Richter, and S. Tomsovic, Phys. Rev. Lett. **123**, 215302 (2019).